

# Optimizing the Thulium Doped Fiber Amplifier (TDFA) gain and noise figure for S-band 16x10 Gb/s WDM systems

Abdel Hakeim. M. Husein  
Physics Department  
Al-Aqsa University  
Gaza, Gaza Strip, Palestine  
hakeim00@yahoo.com

Fady I. El-Nahal  
Department of Electrical Engineering  
Islamic University of Gaza  
Gaza, Gaza Strip , Palestine  
fnahal@iugaza.edu.ps

**Abstract**— This paper aims to evaluate a comprehensive numerical model based on solving rate equations of a thulium-doped silica-based fiber amplifier. The pump power and thulium-doped fiber (TDF) length for single-pass Thulium-Doped Fiber Amplifiers (TDFA) are theoretically optimized to achieve the optimum Gain and Noise Figure (NF) at the center of S-band region. The 1064 nm pump is used to provide both ground-state and excited state absorptions for amplification in the S-band region. The theoretical result is in agreement with the published experimental result.

**Index Terms:** Thulium-Doped Fiber Amplifiers, Rate Equations, Gain, Noise Figure

## I. INTRODUCTION

Increasing demands on the capacity of WDM transmission system now require newly developed transmission windows beyond the amplification bandwidth supported by erbium-doped fiber amplifiers (EDFA's). Due to the tremendous increase in communication traffic in recent years, more and more efforts in research have been directed towards developing highly efficient broad-band fiber amplifier that fully exploit the low-loss band of silica fiber at 1450 nm – 1525 nm range which has a loss of only 0.25 dB/Km in order to increase the transmission capacity of wavelength division multiplexing (WDM) networks [1, 2].

Thulium-doped fiber amplifier (TDFA) provides high-power optical amplification in the S+ (1450–1480 nm) and S-bands (1480–1530 nm) [3], hence the TDFA is expected to complement C- (1530–1560 nm) and L-band (1560–1580 nm) amplification based on EDFAs in high-capacity dense wavelength division multiplexed (DWDM) systems [4,5]. The additional bandwidth, modularity, inherent higher pumping efficiency, and lower nonlinear signal degradation (compared with alternatives such as S-band Raman amplification [6,7]) offered by TDFA enables applications such as coarse wavelength-division multiplexing (CWDM) and fiber to the home (FTTH).

The TDFA length and Pump power are the important parameters that determine the achievable gain and NF in

TDFA [8]. In this paper, we detail the observation and modeling of TDFA where TDFA gain and NF are optimized by solving the rate equations.

## II. CONFIGURATION OF THE TDFA

The basic architecture used to model TDFA in the WDM system is shown in Fig. 1. The system consists of 16 input signals (channels), an ideal multiplexer, a pump laser, pump coupler, Thulium-doped fiber (TDF), Optical spectrum analyzer and dual port WDM analyzer. The structural design shows the setup of the single pass TDFA. The input of the system is 16 equalized wavelength multiplexed signals (channels) in the wavelength region of 80 nm (1450 nm-1530 nm) with 5 nm channels spacing. The power of each channel is -20 dBm. The pumping at 1064 nm is used to excite the doped atoms to a higher energy level. The TDF used is a glass based one with thulium density of  $15.6 \times 10^{24} m^{-3}$ , core radius is  $1.3 \mu m$ , doping radius is  $1.3 \mu m$  and Numerical aperture (NA) is 0.3. The simulation done with maximum number of iterations is 150 and relative error is  $5 \times 10^{-4}$ .

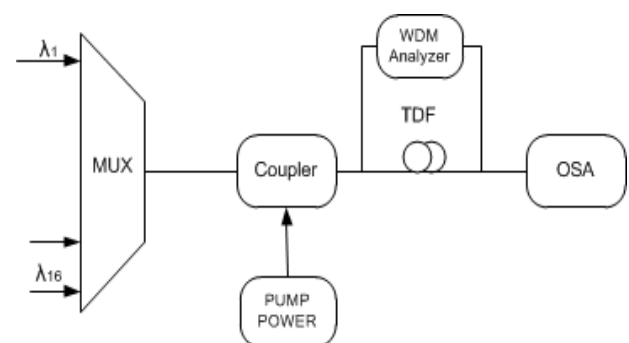


Figure 1. Thulium-doped fiber amplifier layout.

### III. THEORY OF THE TDFA

The rate equations describe the interaction between signal, pump, and ASE light in the TDFA. The rate equations are used to analyze theoretically the populations in the energy levels of  $\text{Tm}^{3+}$  ions under 1064 nm pump and signal power conditions. The absorption and stimulated emission cross sections define the absorption coefficient for pump light and gain coefficient for signal light [9]. The transition cross-sections of thulium are shown in Fig. 2 [8]. The transition cross-sections were calculated in fluoride based TDF [10]. The Judd–Ofelt analysis shows that the transition strengths obtained were consistent with those for silica.

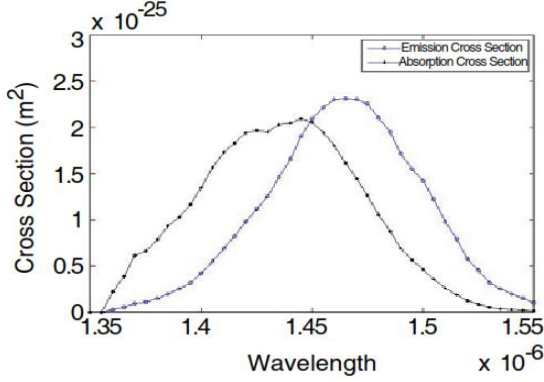


Figure 2. Absorption and emission cross-sections spectra of the fluoride-based TDFA.

An analysis of a six energy levels system is shown in Figure 3, where the energy levels of trivalent thulium ion in fluoride glass are displayed. The absorption and emission transitions are shown in fig. 3 (a) and (b), respectively for the TDFA with 1064 nm pump wavelength. For S-band amplification, the main transition is from  ${}^3H_4 \rightarrow {}^3F_4$  energy levels. Pumping at 1064 nm range takes benefit of the excited state absorption (ESA)  ${}^3F_4$  at the level to excite electrons to the upper energy state. On the other hand, as 1064 nm is the main source of excitation, ground state absorption (GSA) of 1064 nm and /or WDM signals at the  ${}^3H_6$  ground state must be nonzero in order to populate  ${}^3H_5$  energy level and then relaxed to the  ${}^3F_4$  energy level by non-radiative decay [11]. By exciting the TDFA at a fixed level (at 1064 nm), increasing the input WDM signals power further populates the lower energy state ( ${}^3F_4$ ), from which the excited ions are raised to the upper energy state ( ${}^3H_4$ ) because of excess pump power [11]. The pumping transition  ${}^3F_4 \rightarrow {}^1G_4$  is (ESA). The energy level of the  ${}^3F_2$  and  ${}^3F_3$  are very close nearly the same and can be regarded as one level for simplicity. So the  ${}^3F_4$  energy level ions are re-excited to the  ${}^3F_2$  energy level and experience non-radiative decay to the  ${}^3H_4$  energy level via excited state absorption [12, 13].

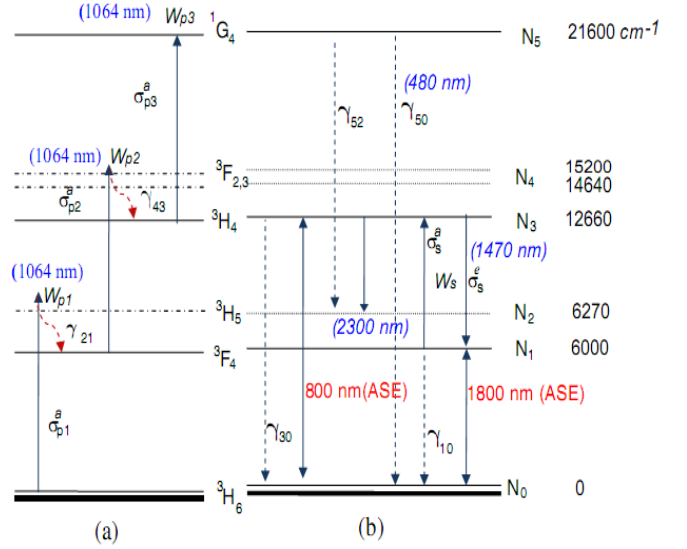


Figure 3. Energy levels with pumping mechanism 1064 nm of trivalent ion ( $\text{Tm}^{3+}$ ) in fluoride glass. (a) Pump absorption, (b) signal and ASE emission transitions.

The Thulium doped fiber ions can be considered homogeneously broadened in amplification system and also characterized by the variables  $N_0, N_1, N_2, N_3, N_4$  and  $N_5$  which are used to represent population ions in the  ${}^3H_6$ ,  ${}^3F_4$ ,  ${}^3H_5$ ,  ${}^3H_4$ ,  ${}^3F_2$ , and  ${}^1G_2$  energy levels, respectively. For simplicity,  $\gamma_{31}$  and  $\gamma_{32}$  are ignored because they are very small compared with  $\gamma_{30}$ .  $\gamma_{51}$  and  $\gamma_{53}$  are also ignored because they are small compared with  $\gamma_{50}$  and  $\gamma_{52}$ .  $\gamma_{20}$  and  $\gamma_{4j}$  ( $j = 0, 1, 2$ ) are very small and can be disregarded because  $\gamma_{21}$  and  $\gamma_{43}$  are multiphonon decay. On the basis of the energy level diagram as in Fig. 3. The rate equation for  $\text{Tm}^{3+}$  population density can be written as follows [14]:

$$\frac{dN_0}{dt} = -W_{p1}N_0 + \gamma_{10}N_1 + \gamma_{30}N_3 + \gamma_{50}N_5 \quad (1)$$

$$\frac{dN_1}{dt} = -(\gamma_{10} + W_{p2} + W_s)N_1 + \gamma_{21}N_2 + W_sN_3 \quad (2)$$

$$\frac{dN_2}{dt} = W_{p1}N_0 - \gamma_{21}^{nr}N_2 + \gamma_{52}N_5 \quad (3)$$

$$\frac{dN_3}{dt} = W_sN_1 - (\gamma_{30} + W_{p3} + W_s)N_3 + \gamma_{43}N_4 \quad (4)$$

$$\frac{dN_4}{dt} = W_{p2}N_1 - \gamma_{43}^{nr}N_4 \quad (5)$$

$$\frac{dN_5}{dt} = W_{p3}N_3 - (\gamma_{50} + \gamma_{52})N_5 \quad (6)$$

$$N_t = \sum_{i=1}^5 N_i \quad (7)$$

where  $W_{p1}, W_{p2}$ , and  $W_{p3}$  are transition rates of  ${}^3H_6 \rightarrow {}^3H_5$ ,  ${}^3H_4 \rightarrow {}^3F_2$ , and  ${}^3F_4 \rightarrow {}^1G_4$  pumping transition. The signal of the central S-band is 1470 nm as signal stimulated absorption and emission is described by transition rate  $W_s$ . The non-radiative transition rate from  ${}^3F_2 \rightarrow {}^3F_4$  and from  ${}^3H_5 \rightarrow {}^3F_4$  energy levels are defined as  $\gamma_{43}^{nr}$ , and  $\gamma_{21}^{nr}$ , respectively.  $\gamma_{ij}$  is the radiative rate from level  $i$  to level  $j$ . Others radiative transitions are not included in the rate equations because they have an ignorable effect on the S-band amplification. For simplicity,  $\gamma_{31}$  and  $\gamma_{32}$  are ignored because they are very small compared with  $\gamma_{30}$ .  $\gamma_{51}$  and  $\gamma_{53}$  are also ignored because they are small compared with  $\gamma_{50}$  and  $\gamma_{52}$ .  $\gamma_{20}$  and  $\gamma_{4j}$  ( $j = 0, 1, 2$ ) are very small and can be disregarded because  $\gamma_{21}$  and  $\gamma_{43}$  are multiphonon decay [15, 16]. Rate equations can be solved by considering the steady state regime where the populations are time independent,  $\frac{dN_i}{dt} = 0$ , ( $i = 0, 1, 2, \dots, 5$ ). The average thulium ion concentration in the core  $N_t$  is calculated by [17]

$$N_t = \frac{2}{b^2} \int_0^{\infty} N(r) r dr \quad (8)$$

where  $b$  is the doping radius, i.e. the half of the concentration profile FWHM. In general, the variable  $N_i$  is functions of position  $r$ ,  $z$  and time  $t$ .  $N(r)$  is the thulium ions concentration profile.  $N_2$  and  $N_4$  are very small compared to other  $N_i$  values. Therefore the total population density  $N_t$  is expressed as:

$$N_t = N_0 + N_1 + N_3 + N_5 \quad (9)$$

The transition rates, which describe the interaction of the electromagnetic field with the  $Tm^{3+}$  ions for a TDFA can be written as [14]:

$$W_{p1} = \frac{P_p \sigma_{p1}^a}{h\nu_p} \quad (10)$$

$$W_{p2} = \frac{P_p \sigma_{p2}^a}{h\nu_p} \quad (11)$$

$$W_{p3} = \frac{P_p \sigma_{p3}^a}{h\nu_p} \quad (12)$$

$$W_s = \frac{P_s \sigma_s^a}{h\nu_s} \quad (13)$$

where  $P_p$  is the pump power intensity and  $P_s$  is the signal power intensity.  $\sigma_{p1}^a$ ,  $\sigma_{p2}^a$ , and  $\sigma_{p3}^a$  are  ${}^3H_6 \rightarrow {}^3H_5$ ,  ${}^3H_4 \rightarrow {}^3F_2$ , and  ${}^3F_4 \rightarrow {}^1G_4$  stimulation absorption

cross sections where the  $Tm^{3+}$  ions are excited homogeneously across the fiber cross-section. So;

$$\gamma_{30} = 1/\tau_3 \quad (14)$$

$$\gamma_{10} = 1/\tau_1 \quad (15)$$

where  $\tau_3$  and  $\tau_1$  are the lifetimes of the  ${}^3F_4$  and  ${}^3H_4$  levels, respectively.  $h$  is the Planck constant,  $\nu_p$  is pump light frequency and  $\nu_s$  is signal light frequency. The light wave propagation equations along the thulium fiber in the  $z$ -direction can be recognized as follows [8]:

$$\frac{dP_p}{dz} = -\Gamma_p (\sigma_{p1} N_0 - \sigma_{p2} N_1 - \sigma_{p3} N_3) P_p - \alpha P_p \quad (16)$$

$$\frac{dP_s}{dz} = \Gamma_s (\sigma_s^e N_3 - \sigma_s^a N_1 - \sigma_{01} N_0) P_s - \alpha P_s \quad (17)$$

$$\frac{dP_{ASE}}{dz} = \pm \Gamma_{ASE} (\sigma_s^e N_3 - \sigma_s^a N_1 - \sigma_{01} N_0) P_{ASE} \pm \Gamma_{ASE} 2h\nu\Delta\nu\sigma_s^e N_3 \mp \alpha P_{ASE} \quad (18)$$

where  $\alpha$  is the background scattering loss which assumed to constant for all wavelength.  $P_{ASE}$  is the amplified spontaneous emission (ASE) at S- band in forward (+) and backward (-) directions along the fiber.  $\sigma_{01}$  is transition cross section from background level  $N_0$  to the first level  $N_1$  for 1800 nm wavelength.  $\Gamma_{s,p,ASE}$  is the overlapping factor between each radiation and the fundamental mode for the signal, the pump, and ASE respectively,  $\Gamma$  can be given by [15,18]:

$$\Gamma = 1 - e^{-\frac{2b^2}{w_0^2}} \quad (19)$$

where  $w_0$  is the model field radius and  $b$  is the thulium ion-dopant radius.

$$w_0 = a \left( 0.761 + \frac{1.237}{V^{1.5}} + \frac{1.429}{V^6} \right) \quad (20)$$

where  $a$  is the core diameter,  $V$  is the normalized frequency. In eq. (17) the term  $\sigma_{01} N_0$  is ignored because the  $\sigma_{01}$  is very small, so eq. (17) becomes as:

$$\frac{dP_s}{dz} = \Gamma_p (\sigma_s^e N_3 - \sigma_s^a N_1) P_s - \alpha P_s \quad (21)$$

The gain ( $G$ ) is given by integration eq. (21) along  $z$ -direction from 0 to  $L$ ;

$$G = \frac{P_s(L)}{P_s(0)} = \exp[\Gamma_p (\sigma_s^e N_3 - \sigma_s^a N_1) L] - \exp(\alpha L) \quad (22)$$

where  $L$  is the length of the TDFA. The gain in decibel (dB) can be written as

$$G(\text{dB}) = 10 \log_{10} \left[ \exp[\Gamma_s (\sigma_s^e N_3 - \sigma_s^a N_1) L] - \exp(\alpha L) \right] \quad (23)$$

From a practical point of view, the noise figure ( $NF$ ) characteristic is very important in an optical amplifier's performance. The rate equation analysis predicts a low-noise characteristic in the optical amplification. Therefore, the  $NF$  was calculated using fiber by an optical method [19].  $NF$  is given by

$$NF = \frac{1}{G} + \frac{P_{ASE}^{out}(\lambda_s)}{G h \nu \Delta \nu} \quad (24)$$

where  $P_{ASE}^{out}(\lambda_s)$  is the output ASE spectral density (W/Hz) at the signal wavelength. For each signal wavelength, the  $NF$  in dB is given by:

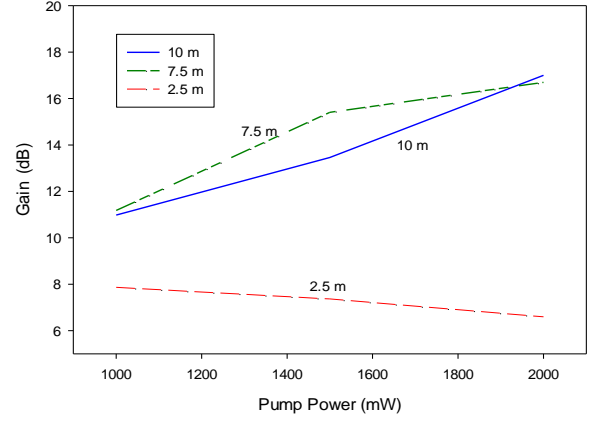
$$NF(\text{dB}) = 10 \times \log_{10} \left[ \frac{1}{G} + \frac{P_{ASE}^{out}(\lambda_s)}{G h \nu \Delta \nu} \right] \quad (25)$$

#### IV. RESULT AND DISCUSSION

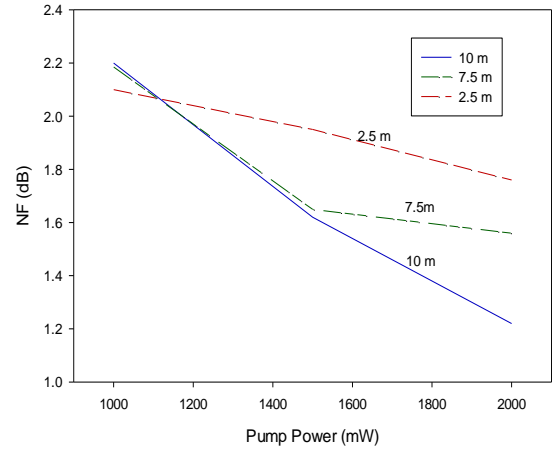
The proposed system amplifies a set of 16 channels in the S-band going from 1450 nm to 1525 nm. The parameters used in the simulation are listed in table 1.

Table 1: Parameters used in the simulation [12]:

Parameter	Value
Thulium ion density	$1.68 \times 10^{25} \text{ 1/m}^3$
Numerical aperture	0.4
Fiber Length	2.5, 7.5, 10 m
Core radius	$1.3 \mu\text{m}$
Background loss type	Constant
Nonradiative lifetime of Tm energy level 1 ( $1/\gamma_{10}^{nr}$ )	$430 \times 10^{-6} \text{ s}$
Nonradiative lifetime of thulium energy level 2 ( $1/\gamma_{21}^{nr}$ )	$45 \times 10^{-6} \text{ s}$
Nonradiative lifetime of Tm. energy level 3 ( $1/\gamma_{32}^{nr}$ )	$784 \times 10^{-6} \text{ s}$
Radiative trans. rate from level 1 to level 0 $\gamma_{10}$	$285.7 \text{ s}^{-1}$
Radiative trans. rate from level 3 to level 0 $\gamma_{30}$	$1353.83 \text{ s}^{-1}$
Radiative trans. rate from level 5 to level 0 $\gamma_{50}$	$581.4 \text{ s}^{-1}$
Radiative transition rate from level 5 to level 2 $\gamma_{52}$	$384.84 \text{ s}^{-1}$



(a) Gain



(b) NF

Figure 4. Gain and Noise Figure (NF) versus pump power at different lengths  $L=2.5\text{m}$ ,  $7.5\text{m}$  and  $10\text{m}$ .

Optimization of the length of the thulium-doped fiber (TDF) is one of the most important issues for optical networks that need to be considered for designing a TDFA in order to obtain the best gain with the lowest noise figure. The gain and noise figure of the TDFA are dependent on the TDF length and the operating pump power. The TDF length is selected carefully, when the TDF length is too short, the TDFA will be saturated at a low pump power and this does not provide a high gain. For a short TDF, the total population is very low and therefore the TDF is fully inverted by a low amount of pump power. When this low amount of pump power is used then the optimized TDF length is short. The length of the TDF is optimized by calculating the gain as a function of TDF length for various operating pump powers. The input signal

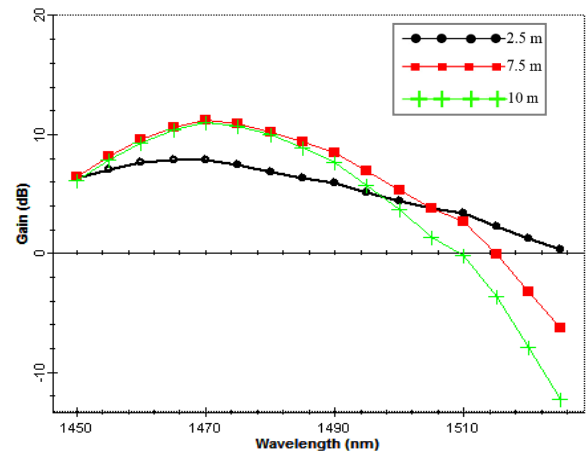
power and wavelength is fixed at  $-20$  dBm and  $1470$  nm, respectively and the pump power is varied from  $1000$  mW to  $2000$  mW.

Three different amplifier lengths are simulated ( $2.5$  m,  $7.5$  m,  $10$  m) and the gain and NF curves are plotted in Figure 4. It is clear from the results that the gain increases with increasing the pump power for  $L = 7.5$  m and  $10$  m and it stays almost constant at  $L = 2.5$  m. However, the best gain is achieved at  $L = 7.5$  m. For the NF results, it is clear that increasing the pump power and the fiber length has a little impact on the NF.

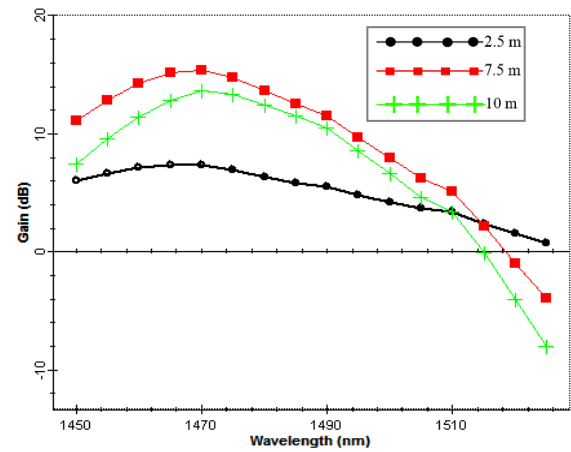
Although the  $10$  m long TDFA design provides the highest gain ( $16.7$  dB) at pump power of  $2000$  mW. However the use of a high pump power is in conflict with the main objective of the TDFA design which requires a smaller pump power especially for long haul applications. For this reason, a very long TDF is not recommended to be considered as a reference TDF length during the design of single pass TDFAs. In the optical network, an amplifier is mainly designed to obtain a gain as high as possible with a low noise figure using a minimum pump power. So the optimum length is  $7.5$  m with optimum pump power of  $1500$  mW, where a gain of  $15.4$  dB and NF of  $2.9$  dB are achieved.

Figure 5 shows the gain versus signal wavelength at different lengths  $2.5$  m,  $7.5$  m, and  $10$  m with different pump powers of  $1000$  mW,  $1500$  mW and  $2000$  mW respectively. At  $10$  m length of TDFA with pump power  $1000$  mW,  $1500$  mW and  $2000$  mW the maximum value of the gain is found  $10.98$  dB,  $13.64$  dB, and  $17$  dB, respectively. At the pump power  $1000$  mW,  $1500$  mW and  $2000$  mW the gain of TDFA at length of amplifier  $7.5$  m is archived and found  $11.18$  dB,  $15.41$  dB, and  $16.7$  dB, respectively. At the length  $2.5$  m the maximum gain is found  $7.87$  dB,  $7.37$  dB, and  $6.6$  dB, respectively. Figure 5 shows that the maximum gain is achieved at the center of S-band ( $1470$  nm) channel 12. It is clear from the figure that the gain increases with increasing signal wavelength from  $1450$  nm to  $1470$  nm then decreases to the minimum at  $1530$  nm. Moreover, it is noted from the figure that the maximum gain at the center wavelength ( $1470$  nm) is achieved at length of  $7.5$  m for different pump powers. However at pump power of  $2000$  mW the maximum gain at the center wavelength is approximately the same at  $7.5$  m and  $10$  m.

Fig. 6 shows the noise figures against input signal wavelength with power  $-20$  dBm at different pump power at different TDFA lengths. At  $2.5$  m length the value of NF is considered high with the gain dB and is found at the center of S-band  $1470$  nm (channel 12),  $3.95$  dB,  $3.51$  dB, and  $3.12$  for  $1000$  mW,  $1500$  mW and  $2000$  mW pump powers, respectively as shown in figures 6a- c. It is noted that at the center of S-band with TDFA length of  $7.5$  m the value of NF is  $6.39$  dB,  $7.6$  dB and  $7.4$  dB for  $1000$  mW,  $1500$  mW and  $2000$  mW pump powers, respectively. While the NF values at  $10$  m TDFA length and at center S-band  $1470$  nm channel 12 are  $12.9$  dB,  $10.18$  dB and  $9.27$  dB for  $1000$  mW,  $1500$  mW and  $2000$  mW pump powers, respectively. The NF fluctuates with increasing the signal wavelength as shown in the figure 6.



(a)



(b)

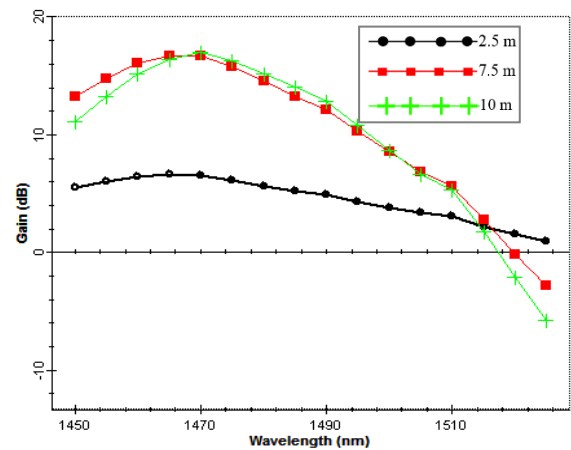
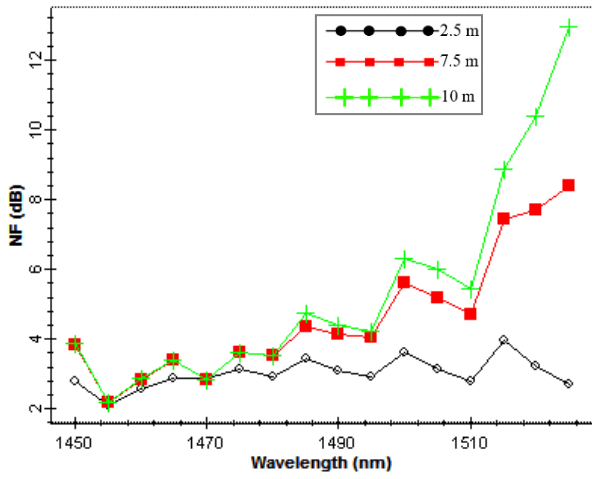
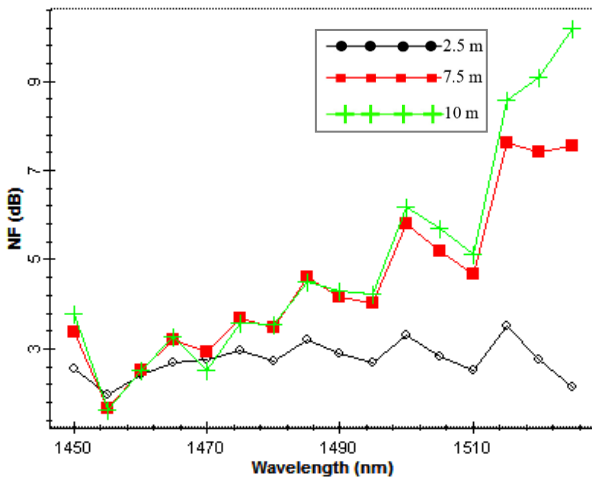


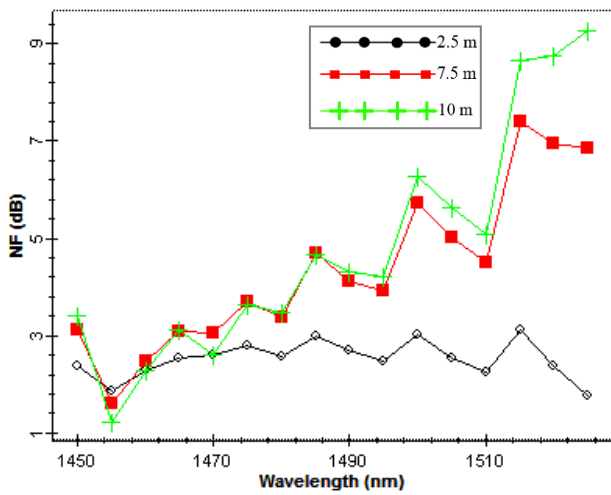
Figure 5. Gain versus signal wavelength at different lengths with pump power of a)  $1000$  mW, b)  $1500$  mW, and c)  $2000$  mW.



(a)

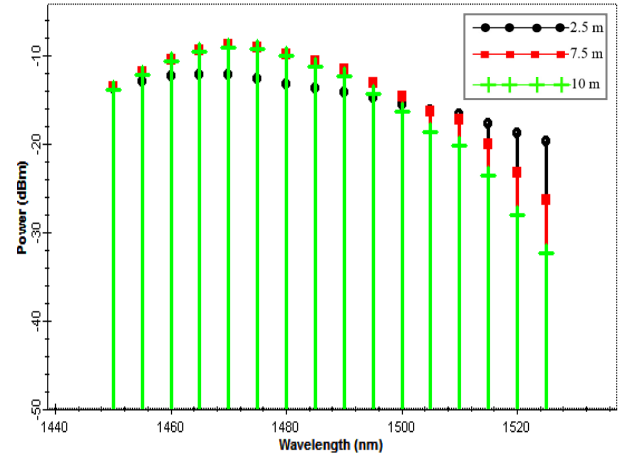


(b)

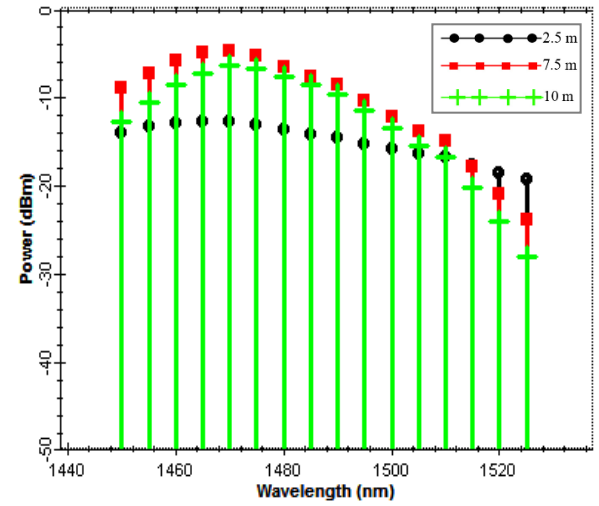


(c)

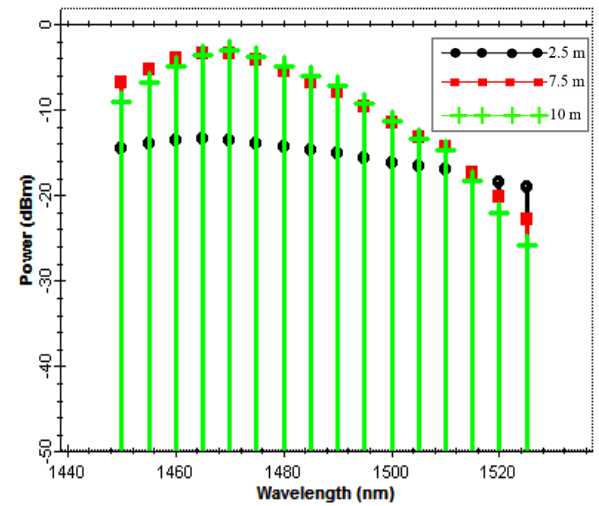
Figure 6. NF versus signal wavelength at different lengths at pump power of a) 1000 mW, b) 1500mW, and c) 2000mW.



(a)



(b)



(c)

Fig. 7: The output spectrum at different lengths at pump power of a) 1000 mW, b) 1500mW, and c) 2000mW

The output signal wavelength spectrum is shown in figure 7 for different input pump power with different length. The power is increasing from 1450 nm to reach the maximum value at the center of S-band 1470 nm then decreasing to reach the minimum value at channel 16. At the center channel 12, the signal power at 1500 mW and 2000 mW nearly the same for different lengths of TDFA amplifier.

## V. CONCLUSION

This paper has described in detail the relation between the operating 1064 nm pump power and TDFA length for single-pass TDFA. The simulation results are based on the rate equations to determine the gain and noise figures for TDFA. The simulated model was also used for optimizing of the TDFA parameters: fiber length, pump wavelength and pump power. The theoretical results obtained here is in agreement with the published experimental result. It is found that the optimum TDFA length is 7.5 m with optimum pump power of 1500 mW. The results show that silica-based TDFA amplifiers are interesting comparing to its competitors within the S-band optical amplifiers, namely the fluoride-fiber based TDFA and the Raman amplifiers.

## REFERENCES

- [1] Bumki Min, Hosung Yoon, Won Jae Lee, and Namkyoo Park, "Coupled Structure for Wideband EDFA with Gain and Noise Figure Improvement from C to L-band ASE Injection," *IEEE Photon. Technol. Lett.*, vol. 12, pp. 480482, May 2000.
- [2] J. Kani, M. Jinno, "Wideband and flat-gain optical amplification from 1460 to 1510nm by serial combination of a thulium-doped fluoride fiber amplifier and fiber-Raman amplifier," *Electron. Lett.*, vol. 35, pp. 1004-1006, 1999.
- [3] Scott S. H. Yam and Jaedon Kim "Ground State Absorption in Thulium-Doped Fiber Amplifier: Experiment and modeling." *IEEE journal of selected topics in quantum electronics*, vol. 12, no. 4, pp 797-803, 2006.
- [4] T. Ito, K. Fukuchi, K. Sekiya, D. Ogasawara, R. Ohhira, and T. Ono, "6.4 Tb/s (160×40 Gb/s) WDM transmission experiment with 0.8 bit/s/Hz spectral efficiency," presented at the Eur. Conf. Optical Communications, Munich, Germany, 2000, Paper PDP1.1.
- [5] S.Bigo, A. Bertaina, Y. Frignac, S. Borne, L. Lorcy, D. Harnoir, D. Bayart, J. P. Hamaide, W. Idler, E. Lach, B. Franz, G. Veith, P. Sillard, L. Fleury, P. Guenot, and P. Nouchi, "5.12 Tb/s (128×40 Gb/s WDM) transmission over 3×100 km of TeraLight™ fiber," presented at the Eur. Conf. Optical Communications, Munich, Germany, 2000, Paper PDP1.2.
- [6] S. S.-H. Yam, M. E. Marhic, T. Sakamoto, E. S.-T. Hu, Y. Akasaka, and L. G. Kazovsky, "Comparison of four wave mixing and cross phase modulation in thulium doped fiber amplifier and S-band discrete Raman amplifier," in *Proc. OECC*, Yokohama, Japan, Jun. 2002, pp. 9D1-9D4.
- [7] Bumki Min, Won Jae Lee, and Namkyoo Park, "Efficient Formulation of Raman Amplifier Propagation Equations with Average Power Analysis," *IEEE Photon. Technol. Lett.*, to appear in November 2000 issue.
- [8] S. D. Emami and S. W. Harun "Optimization of the 1050 nm pump power and fiber length in single-pass and double-pass thulium doped fiber amplifiers" *Progress in Electromagnetics Research B*, Vol. 14, pp 431-448, 2009.
- [9] Kasamatu, T., Y. Yano, and T. Ono, "1.49 μm band gain-shifted thulium doped fiber amplifier for WDM transmission system," *Journal of Lightwave Technol.*, Vol. 20, No. 10, 1826-1838, 1998.
- [10] Guy, S., W. Meffre, A.M. Jurduc, B. Jacquier, F. Roy, P. Baniel, D. Bayart, A.L. Sauze, C. Collet and J.J. Girard. In: *In Tech. Digest of OAA'01*, Stresa, Italy, July 1-4, paper OWB5, 2001.
- [11] Scott S. H. Yam and Jaedon Kim "Ground State Absorption in Thulium-Doped Fiber Amplifier: Experiment and modeling." *IEEE journal of selected topics in quantum electronics*, vol. 12, no. 4, pp 797-803, 2006
- [12] Peterka, P., B. Faure, W. Blance, and M. Karasek, "Theoretical modeling of S-band thulium doped silica fiber amplifiers," *Optical and Quantum Electronics*, Vol. 36, pp 201-212, 2004.
- [13] Lee, W. J., B. Min, J. Park, and N. Park, "Study on the pumping wavelength dependency of S/S+-band fluoride based thulium doped fiber amplifiers," *Optical Fiber Communication Conference and Exhibition*, OFC 2001, Vol. 2, TuQ5-1-TuQ5-4, 2001.
- [14] T. Komukai, T. Yaoto, T. Sugawa, and Y. Miyajima, "Upconversion pumped thulium-doped fluoride fiber amplifier and laser operating at 1.47 μm," *IEEE J. Quantum Electron.*, vol. 31, no. 11, pp. 1880-1889, 1995.
- [15] J. Sanz, R. Cases, and R. Alcalá, "Optical properties of Tm<sup>3+</sup> in fluorozirconate glass." *J. Non-Crystalline Solids*, vol. 93, pp. 377-386, 1987.
- [16] C. Guery, J. L. Adam, and J. Lucas, "Optical properties of Tm<sup>3+</sup> ions in indium-based fluoride glasses," *J. Luminescence*, vol. 42, pp. 181-189, 1988
- [17] Desurvire, E., "Erbium-Doped Fiber Amplifiers: Principles and Applications", John Wiley & Sons, New York, 1994.
- [18] Michael, J. and F. Dignonnet, *Rare-earth-doped Fiber Lasers and Amplifiers*, CRC Press, 2001.
- [19] P. R. Morkel and R. I. Laming, "Theoretical modeling of erbium-doped fiber amplifiers with excited-state absorption." *Opt. Lett.*, vol. 14, no. 19, pp. 1062-1064, 1989.